Proc. Natl. Acad. Sci. USA
Vol. 91, pp. 7970–7974, August 1994
Biochemistry

Kinetics and mechanism of autoprocessing of human immunodeficiency virus type 1 protease from an analog of the Gag–Pol polyprotein

JOHN M. LOUIS*, NASHAAT T. NASHED†‡, KEVIN D. PARRIS§, ALAN R. KIMMEL*, AND DONALD M. JERINA†

*Laboratory of Cellular and Developmental Biology, †Laboratory of Bioorganic Chemistry, and §Laboratory of Molecular Biology, National Institute of Diabetes and Digestive and Kidney Diseases, National Institutes of Health, Bethesda, MD 20892

Communicated by David R. Davies, March 11, 1994

ABSTRACT **Upon renaturation, the polyprotein MBP-ΔTF-Protease-ΔPol, consisting of HIV-1 protease and short native sequences from the trans-frame protein (ΔTF) and the polymerase (ΔPol) fused to the maltose-binding protein (MBP) of *Escherichia coli*, undergoes autoprocessing to produce the mature protease in two steps. The initial step corresponds to cleavage of the N-terminal sequence to release the protein intermediate Protease-ΔPol, which has enzymatic activity comparable to that of the mature enzyme. Subsequently, the mature enzyme is formed by a slower cleavage at the C terminus. The rate of increase in enzymatic activity is identical to that of the appearance of MBP-ΔTF and the disappearance of the MBP-ΔTF-Protease-ΔPol. Initial rates are linearly dependent on the protein concentration, indicating that the N-terminal cleavage is first-order in protein concentration. The reaction is competitively inhibited by pepstatin A and has a pH rate profile similar to that of the mature enzyme. These results and molecular modeling studies are discussed in terms of a mechanism in which a dimeric full-length fusion protein must form prior to rate-limiting intramolecular cleavage of the N-terminal sequence that leads to an increase in enzymatic activity.**

Autoprocessing of the viral Gag–Pol polyprotein is an essential step in the life cycle of RNA viruses and retroviruses (1, 2), including human immunodeficiency virus (HIV). Specific cleavages of the polyprotein are required to release the structural and functional proteins needed for viral maturation. The aspartic protease of HIV-1 is encoded as a part of the Gag–Pol polyprotein (Pr165) and is translated in the Pol reading frame. The mature protease liberated via autoprocessing is responsible for the processing of the polyprotein (3–5) and is catalytically active only as a dimer consisting of two identical subunits (1, 2, 6). Each polypeptide chain contributes one of the two active-site aspartic residues essential for enzymatic activity. Thus, it is presumed that the protease domain in the HIV-1 Gag–Pol polyprotein must initially fold into a conformation similar to that of the mature enzyme and dimerize before the required hydrolysis of peptide bonds can occur. The Gag–Pol polyprotein contains seven cleavage sites, which have complicated the investigation of the kinetics of the autoprocessing reaction. Thus, we have expressed and characterized a fusion protein, MBP-ΔTF-Protease-ΔPol, consisting of HIV-1 protease with a 12-aa sequence from the trans-frame protein (ΔTF) at the N terminus and a 19-aa sequence from the native Pol protein (ΔPol) at the C terminus, fused to the *Escherichia coli* maltose-binding protein (MBP). This fusion protein contains only two cleavage sites, at the N and C termini of the protease domain (5). The time-dependent autoprocessing of this polyprotein provides a simple model for maturation of HIV-1 protease. In this paper, we report the kinetics and propose a mechanism for the processing of HIV-1 protease from this model polyprotein.

The publication costs of this article were defrayed in part by page charge payment. This article must therefore be hereby marked "*advertisement*" in accordance with 18 U.S.C. §1734 solely to indicate this fact.

MATERIALS AND METHODS

MBP-ΔTF-Protease-ΔPol, MBP, and the mature HIV-1 protease were obtained as described (5). MBP-ΔTF-Protease-ΔPol was further purified by size-exclusion column chromatography [Superose 12 RH, 1 cm × 30 cm; Pharmacia LKB], eluted as an oligomer (apparent molecular mass, 1.1×10^6 Da) with 50 mM Tris buffer, pH 8.0/25 mM NaCl/1 mM dithiothreitol/1 mM EDTA, and stored as a stock solution of 460–620 μg/ml. Unless otherwise indicated, all reactions were carried out at 25°C in 100 mM acetate buffer, pH 5.0/5 mM dithiothreitol/5 mM EDTA/0.05% reduced Triton X-100. The pH rate profile was determined at 25°C in 100 mM sodium acetate, Mes, and Mops containing 100 mM NaCl, 5 mM dithiothreitol, 5 mM EDTA, and 0.05% reduced Triton X-100. Rate constants, pK_a, and K_i were determined by fitting the appropriate equation to the data by use of the curve-fitting program ENZFITTER (Biosoft, Cambridge, U.K.).

Kinetic Measurements of Autoprocessing. MBP-ΔTF-Protease-ΔPol (460 μg/ml) was incubated in the presence of 5 mM dithiothreitol and 5 mM EDTA at 25°C for 45 min and denatured by adding an equal volume of 10 M urea. After 10 min, the reaction was initiated by diluting the denatured protein solution 11-fold with buffer. Aliquots of 19 μl were removed at various time intervals and added to 7.5 μl of 4× Laemmli sample buffer to terminate the reaction (5). The samples were analyzed by SDS/PAGE, and the protein bands were visualized by staining with Coomassie brilliant blue G-250 or immunoblotting using antiserum specific to the protease (5). Intensities of the bands were quantified by densitometry. Control experiments showed that the intensities of the stained protein bands on the gels were linearly dependent on the amount of protein. The peptide substrate for HIV-1 protease, Lys-Ala-Arg-Val-Nle-Phe(*p*-NO_2)-Glu-Ala-Nle-NH_2 [American Peptide Company, Santa Clara, CA (7)], was used to assay for enzymatic activity at a concentration of 400 μM [ε_{280} = 12,000 for the *p*-nitrophenyl chromophore (8)]. The reaction was monitored by following the decrease in absorption at 310 nm. In a typical assay, an aliquot of 110 μl of autoprocessing reaction mixture was placed in a microspectrophotometric cell preequilibrated at

Abbreviations: MBP, *Escherichia coli* maltose-binding protein; HIV, human immunodeficiency virus; ΔPol, 19-amino acid native Pol sequence; ΔTF, 12-amino acid sequence from the trans-frame protein; MBP-ΔTF-Protease-ΔPol, polyprotein containing ΔTF and ΔPol at the N and C termini of HIV-1 protease, respectively, fused to MBP.

‡To whom reprint requests should be addressed at: National Institutes of Health, Building 8, Room 1A02, Bethesda, MD 20892.

25°C, and the reaction was initiated by the addition of 10–15 μl of a substrate solution in water.

Kinetics of Protein Folding. Protein folding was monitored by following the increase in fluorescence (excitation at 290 nm, emission at 340 nm). In a typical experiment, 185 μl of 100 mM buffer was placed in a fluorimetric cell (100 μl, Hellma, Forest Hills, NY) at 25°C. The folding process was initiated by adding 15 μl of the denatured protein solution in 5.0 M urea.

Kinetics of Intermolecular Cleavage of the N Terminus. The reactions were carried out as described above for autoprocessing at a concentration of 0.35 μM of MBP-ΔTF-Protease-ΔPol, except that the dilution buffer contained 2.2–4.4 μM purified mature HIV-1 protease, and the final pH of the reaction mixture was 5.2.

Modeling. To the crystallographically determined atomic coordinates of the HIV-1 protease dimer, Protein Data Bank entry 3HVP (9), the sequence ΔTF (Gly-Ala-Asp-Arg-Gln-Gly-Thr-Val-Ser-Phe-Asn-Phe) was inserted at the N terminus. The ΔTF sequence was moved into the binding cleft (10) and the torsion angles of residues 1–10 of the protease were altered to allow the added residues (−12 to −1) to fit within the active site. By analogy to pepsinogen structure (11), residues 1–10 were allowed to be flexible. The fragment consisting of residues −3 to 4 was aligned to the structure of the complex of acetyl pepstatin and HIV-1 protease, Protein Data Bank entry 5HVP (12). In the alignment process, the coordinates of the acetyl pepstatin were held fixed and residues −3 to 4 of the ΔTF-Protease were moved until maximum overlap was obtained. This process was accomplished with the program ALIGN (13) and resulted in a rms of 1.4 Å. The model was then visually inspected, and bad contacts were removed by hand (residues 229, 247, and 287 were unacceptably close to the modeled position of the N-terminal peptide residues). Finally, the model was energy minimized (CHARMM-QUANTA, Polygen, Waltham, MA).

RESULTS

Autoprocessing of MBP-ΔTF-Protease-ΔPol. The 52-kDa MBP-ΔTF-Protease-ΔPol fusion protein undergoes a time-dependent reaction to produce the 11-kDa mature HIV-1 protease in two steps. Fig. 1*A* shows the time-dependent cleavage of the 52-kDa fusion protein to release the 39-kDa MBP-ΔTF protein. Fig. 1*B* shows the initial appearance of the 13.2-kDa protease-ΔPol protein fragment and its subsequent conversion to the mature protease. The identities of both proteins were confirmed by comigration with previously characterized proteins (5). The time course for the appearance of the mature enzyme is clearly characterized by a lag period in the early stages of the reaction. This lag period indicates that the mature protease is formed only via a reaction intermediate. Unlike the 13.2-kDa intermediate, the protein fragment MBP-ΔTF-Protease (50 kDa) was not observed during the reaction (Fig. 1*A*). Thus, the major path for the formation of the mature enzyme must be through the 13.2-kDa protein that is produced by the cleavage of the scissile peptide bond at the N terminus of the protease domain.

Kinetics of MBP-ΔTF-Protease-ΔPol Folding. The folding of the MBP-ΔTF-Protease-ΔPol is accompanied by a biphasic fluorescence change. The initial major change occurs too fast to measure and is followed by a first-order process that corresponds to 20–25% of the total fluorescence change. A first-order rate constant (k_{fold}) of 0.52 ± 0.004 min^{-1} was determined from initial-rate measurements, as well as by fitting a first-order equation to data obtained over the total time course of the reaction. A similar first-order process is observed for the folding of purified MBP, k_{fold} = 0.88 ± 0.01 min^{-1}, whereas mature HIV-1 protease folds instantaneously

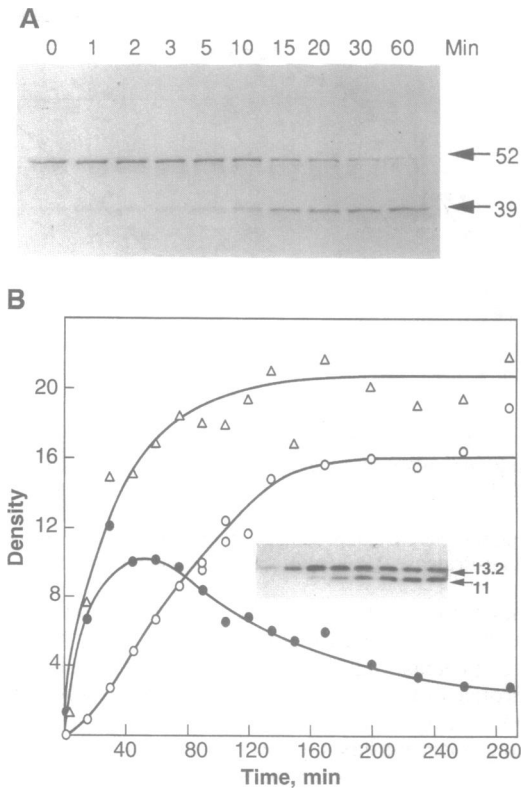

FIG. 1. Time course of the autoprocessing reaction. The protein bands corresponding to MBP-ΔTF-Protease-ΔPol (52 kDa) and MBP-ΔTF (39 kDa) were visualized by staining with Coomassie blue G-250 (*A*), whereas those corresponding to the Protease-ΔPol (13.2 kDa) and the mature protease (11 kDa) were detected by immunoblotting. A typical immunoblot (inset of *B*) shows a part of a time course for the autoprocessing reaction. Lane 1 is at 1 min, lane 2 is at 15 min, and the following lanes are at 15-min intervals. *B* shows a plot of the corrected densities for Protease-ΔPol (●), mature protease (○), and their sum (△) vs. time.

with concomitant recovery of enzymatic activity. For both MBP and the fusion protein, k_{fold} is decreased by a factor of <2 upon raising the urea concentration from 0.37 to 1.5 M (data not shown).

Kinetics of Autoprocessing. The autoprocessing reaction was monitored by following the increase in protease activity, the disappearance of MBP-ΔTF-Protease-ΔPol, and the appearance of MBP-ΔTF. Reaction time courses monitored by the three measurements are identical (Fig. 2). The kinetic order of the reaction was determined from initial rate measurements obtained by following the appearance of enzymatic activity and the disappearance of MBP-ΔTF-Protease-ΔPol. A linear relationship between these initial rates and protein concentration (*Inset* of Fig. 2) indicates that the cleavage of the N terminus is first-order in protein concentration. Thus, a first-order equation was fit to data obtained over the total time course of the reaction. In all cases, good fit is observed for at least three half-lives. The first-order rate constant for the autoprocessing reaction, k_{first}, determined by following the initial rate of increase in enzymatic activity (0.043 ± 0.002 min^{-1}), and the disappearance of MBP-ΔTF-Protease-ΔPol (0.039 ± 0.004 min^{-1}) are in close agreement with those determined from the total time course measured by following the increase in enzymatic activity (0.033 ± 0.003 min^{-1}), the appearance of the MBP-ΔTF (0.040 ± 0.004 min^{-1}) and the disappearance of MBP-ΔTF-Protease-ΔPol (0.036 ± 0.003 min^{-1}).

Denaturation of MBP-ΔTF-Protease-ΔPol in 5 M urea is necessary prior to autoprocessing, since the protein aggregates at high concentrations as indicated by its elution as an

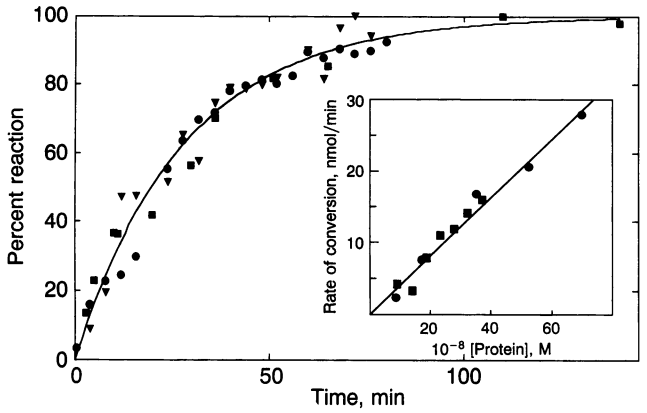

FIG. 2. Time course for the autoprocessing reaction measured by following the increase in enzymatic activity (■), appearance of MBP-ΔTF (▼), and disappearance of MBP-ΔTF-Protease-ΔPol (●). (*Inset*) Dependence of the initial rates of reaction measured by following the increase in protease activity (■), and disappearance of MBP-ΔTF-Protease-ΔPol (●) on protein concentrations.

oligomer from a size-exclusion column. Dilution of the protein without urea treatment results in only 20% of the expected protease activity after 80 min. The denatured MBP-ΔTF-Protease-ΔPol does not appear to reaggregate upon dilution to concentrations between 874 and 87.4 nM. The following observations support this conclusion: (*i*) the first-order kinetics of the autoprocessing reaction, (*ii*) the linear relationship between protein concentration and protease activity attained by autoprocessing after 1 hr (three half-lives), and (*iii*) the complete conversion of the fusion protein to products.

Good first-order kinetics were observed between pH 5.0 to 7.5. The reaction could not be studied below pH 5 due to precipitation of the protein. A plot of k_{first} vs. pH is shown in Fig. 3, and the determined pK_a is 6.68 ± 0.06.

Inhibition of Autoprocessing. Both the substrate used for assay of HIV-1 protease and pepstatin A, a specific inhibitor of aspartic proteases (14), inhibit autoprocessing. The kinetics of inhibition by pepstatin A were examined in detail by analyzing the products by SDS/PAGE. The minimal mechanism

$$[\text{tetrapod-1.I}] \overset{k_i}{\rightleftharpoons} [\text{I}] + [\text{tetrapod-1}]$$

$$\overset{K_T}{\rightleftharpoons} \text{tetrapod} - 2 \overset{k_N}{\rightarrow} \text{products}$$

is proposed to describe the inhibition (see Fig. 4). If all the

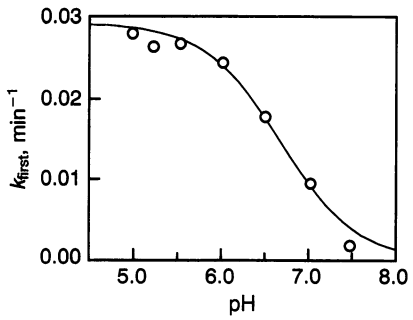

FIG. 3. pH rate profile for k_{first}. Rate constants were determined by following the appearance of MBP-ΔTF and disappearance of MBP-ΔTF-Protease-ΔPol by SDS/PAGE. The line is a theoretical curve for a pK_a of 6.68 (see text) and a limiting rate constant (k_{lim}) at the plateau of 0.029, based on the equation $k_{first} = k_{lim}/(1 + K_a/[H^+])$.

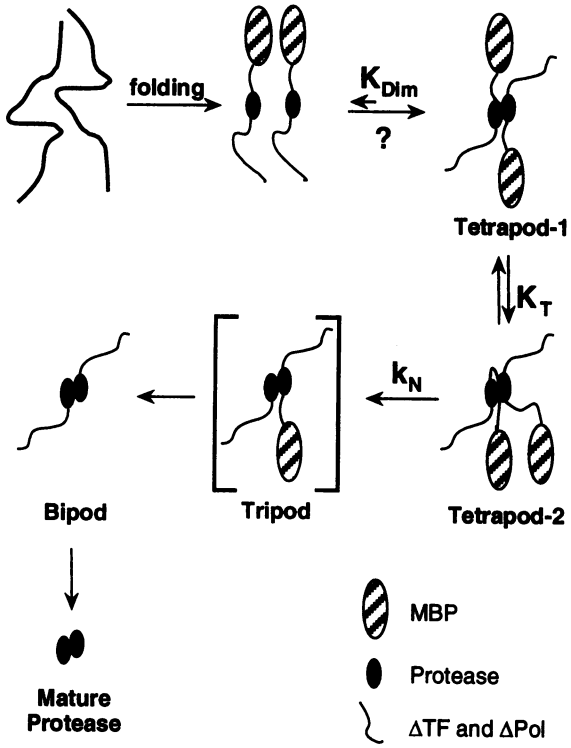

FIG. 4. Proposed mechanism for autoprocessing of HIV-1 protease from the model polyprotein MBP-ΔTF-Protease-ΔPol.

equilibria are fast relative to the step that commits tetrapod-2 for the hydrolysis of the N-terminal peptide bond and if the bulk of the protein is in one of the tetrapod forms, it can be shown that

$$\text{Rate} = k_{obs}[\text{tetrapod}]_{total} \quad [1]$$

$$k_{obs} = k_N/K_T(1 + [\text{I}]/K_i), \quad [2]$$

where $[\text{tetrapod}]_{total}$ and [I] are the concentrations of the total unreacted tetrapod and inhibitor, respectively; k_{obs} is the first-order rate constant, K_T is the equilibrium constant between the two forms of the tetrapod, k_N is the rate constant for cleavage of the N terminus, and K_i is the inhibition constant. When [I] = 0, k_{obs} equals k_N/K_T, which corresponds to k_{first}. Eq. 2 can be rearranged to the linear form

$$1/k_{obs} = K_T/K_N + [\text{I}]K_T/k_N K_i. \quad [3]$$

A plot of $1/k_{obs}$ vs. the concentration of pepstatin A (five measurements between 0 and 810 nM) is a straight line with a slope of (1.46 ± 0.09) × 10^8 min·M^{-1}, an intercept of 28.5 ± 4.6 min, and a correlation coefficient of 0.989. The estimated inhibition constant K_i is 195 ± 44 nM. This K_i is within the range of values of K_i reported for the inhibition of mature HIV-1 protease by pepstatin A (15, 16).

Processing of MBP-ΔTF-Protease-ΔPol by Mature Protease. The mature HIV-1 protease catalyzes the processing of MBP-ΔTF-Protease-ΔPol. The initial cleavage occurs at the N terminus as indicated by a time-dependent appearance and disappearance of the Protease-ΔPol fragment in a fashion similar to that shown in Fig. 1. The kinetics of appearance of the product MBP-ΔTF is characterized by a lag period of ≈3 min, which may result from a requirement for renaturation of the fusion protein prior to its cleavage by the exogenous mature protease. After the lag period, the reaction follows first-order kinetics for at least three half-lives. Since the amount of catalytically active protease—i.e., 13.2 kDa and mature enzyme—formed during the reaction is negligible relative to that of the exogenously added protease, the active

enzyme concentration is essentially unchanged during the reaction. If the concentrations of the added protease and MBP-ΔTF-Protease-ΔPol are below K_m for the mature protease, it can be shown that $k_{obs} = k_{first} + k_{cat}[E]/K_m$, where k_{obs} and [E] are the pseudo-first-order rate constant and the concentration of added enzyme, respectively. A plot of k_{obs} vs. [E] is linear with correlation coefficient of 0.963 and a positive intercept of (0.044 ± 0.008) min^{-1}. The slope of the line is k_{cat}/K_m, (2.9 ± 0.3) × 10^4 $M^{-1} \cdot min^{-1}$.

DISCUSSION

Mechanism of Autoprocessing. The observation that the cleavage of the N terminus of the polyprotein construct exhibits first-order kinetics in protein concentration was somewhat unexpected. Since a protein dimer is required for enzymatic activity (17, 18), a second-order (bimolecular) reaction was anticipated. Dimer formation is required for autoprocessing, since both the pH rate profile and the inhibition with pepstatin A demonstrate that the reaction occurs at an active site of an aspartic protease similar to that of the mature HIV-1 protease. We have not been able to characterize a second-order process that corresponds to dimer formation. Since k_{fold} is ≈15 times larger than k_{first}, protein folding cannot be a rate-limiting step for autoprocessing and should not complicate the kinetics of the subsequent steps. The process represented by k_{fold} cannot be attributed to dimer formation, because it follows first-order kinetics and lacks sensitivity to increasing urea concentration, and the monomeric MBP (19) exhibits a similar process. On the other hand, these results are similar to those obtained for the slowest step in the folding of simple proteins (ref. 20, pp. 311–313; ref. 21), which has been assigned to the cis/trans isomerization of the peptide bond involving the nitrogen of proline (AA-Pro). Since MBP-ΔTF-Protease-ΔPol and MBP contain 33 and 22 AA-Pro peptide bonds, respectively (5, 22), k_{fold} is likely to represent the same process in the present system.

The likely explanation for the observed first-order kinetics of the N-terminal cleavage is that the rate of formation of tetrapod-1 is much faster than the rate of intramolecular cleavage of the N terminus and that most of the folded MBP-ΔTF-Protease-ΔPol is in one of the tetrapod forms (Fig. 4) at the lowest protein concentration used (140 nM). If intermolecular cleavage of the N terminus occurred or dimer formation were rate limiting, a higher kinetic order would have been observed. Since protein domains are known to fold independently (ref. 20, p. 321), the folding of the 99-aa protease domain (1) is expected to be much faster than that of the 370-aa MBP domain (22). Therefore, it is likely that the protease domain folds and dimerizes to form tetrapod-1 before folding of the MBP domain is completed.

The mechanism shown in Fig. 4 is proposed to account for the results presented. The denatured MBP-ΔTF-Protease-ΔPol folds and dimerizes to form tetrapod-1. Competitive inhibition of the autoprocessing reaction by pepstatin A is consistent with the presence of at least two forms of the tetrapod, one of which (tetrapod-1) has a binding site that is similar to that of the mature enzyme. The process represented by k_{first} is dependent on an ionizable group with a pK_a of 6.68 in its protonated form (Fig. 3). This pH rate dependence closely resembles that of k_{cat}/K_m for hydrolysis of various peptide substrates catalyzed by the mature HIV-1 protease (23). Thus, the step represented by k_{first} occurs at an active-site with catalytic groups similar to those of the mature protease. Tetrapod-1 is in equilibrium with its conformational isomer tetrapod-2. The proposed intermediate, tetrapod-2, is analogous to the enzyme-substrate complex in normal enzymatic reactions and has one of its N-terminal strands bound to its own active site. The observation of first-order kinetics for the N-terminal cleavage in the presence of pepstatin A is consistent with equilibria (represented by K_i and K_T) that are rapid relative to the step that commits the tetrapod for the hydrolytic reaction and are therefore not rate limiting. It should be pointed out that dimer formation must be a second-order process, and it could become rate-limiting (17, 18) at a much lower protein concentration.

The cleavage of the N terminus of the tetrapod to generate a tripod must be rate-limiting for the increase in enzymatic activity and formation of the product MBP-ΔTF, as well as for disappearance of MBP-ΔTF-Protease-ΔPol. If the rate of disappearance of the tripod were slower than that of its formation and if the tripod were to accumulate during the reaction, biphasic kinetics with an initial "burst" would be expected for the appearance of the product MBP-ΔTF and disappearance of the MBP-ΔTF-Protease-ΔPol.

Catalytic Activity of Protease Fusion Proteins. A comparison of the reaction time courses in Figs. 1 and 2 shows that the increase in enzymatic activity corresponds to the sum of the 13.2- and 11-kDa proteins. Thus, the 13.2-kDa protein must have enzymatic activity comparable to that of the mature enzyme. This conclusion is further supported by the observation of first-order kinetics with no lag period for the increase in enzymatic activity during autoprocessing.

That the autoprocessing reaction can be monitored by following the increase in protease activity (Fig. 2) demonstrates that tetrapod-1 has low enzymatic activity relative to that of the mature protease or the bipod. Since the substrate for HIV-1 protease binds to tetrapod-1 and inhibits autoprocessing, the low enzymatic activity is not due to the inability of tetrapod-1 to bind the substrate. The observed k_{first} (0.036 min^{-1}) may be compared with the first-order rate constant k_{cat} for the HIV-1 protease-catalyzed hydrolysis of a peptide substrate that corresponds to the N-terminal cleavage site [21 min^{-1} in 50 mM acetate buffer, pH 5.5, at 30°C (24)]. Such a comparison indicates that the tetrapod is 600 times less active than the mature enzyme.

Comparison of the Intra- and Intermolecular Reactions. Due to their different kinetic orders, k_{first} for the intramolecular process cannot be directly compared with k_{cat}/K_m for the intermolecular reaction catalyzed by the mature protease. However, from the relationship $k_{first} = k_{cat}[E_o]/K_m$, the amount of the mature HIV-1 protease that is required to produce a reaction rate equal to that of the intramolecular process is calculated to be 1.4 μM. This amount of enzyme is a measure of the entropic advantage of the intramolecular process over the intermolecular process, even though the tetrapod has much lower intrinsic catalytic activity than the mature enzyme. Under the experimental conditions employed (Figs. 1 and 2), such a concentration of the mature protease was not achieved. A similar consideration may account for the accumulation of the 13.2-kDa intermediate if further cleavage requires intermolecular reaction.

Structure. The ΔTF sequence was modeled bound to the active site of HIV-1 protease (Fig. 5). In this structure, there are no unacceptably close contacts. The ΔTF sequence fits into the protease active site (of tetrapod-2, Fig. 4) with the scissile peptide bond (Phe-Pro) near the active site Asp residues without major reorganization of the protease structure. The model is consistent with our experimental demonstration of an intramolecular mechanism for cleavage of the fusion protein and with the mechanism of autoprocessing postulated by Navia et al. (25) on the basis of the crystal structure of the mature enzyme (25).

Comparison of the Mechanism of Activation of Aspartic Proteases from HIV-1 and Mammals. Comparing the mechanism of conversion of pepsinogen to pepsin (26), a mammalian aspartic protease, with that in Fig. 4 reveals several striking similarities: (*i*) cleavage of the N-terminal strand is required for mature-like protease activity, (*ii*) intramolecular cleavage predominates until a sufficient quantity of the

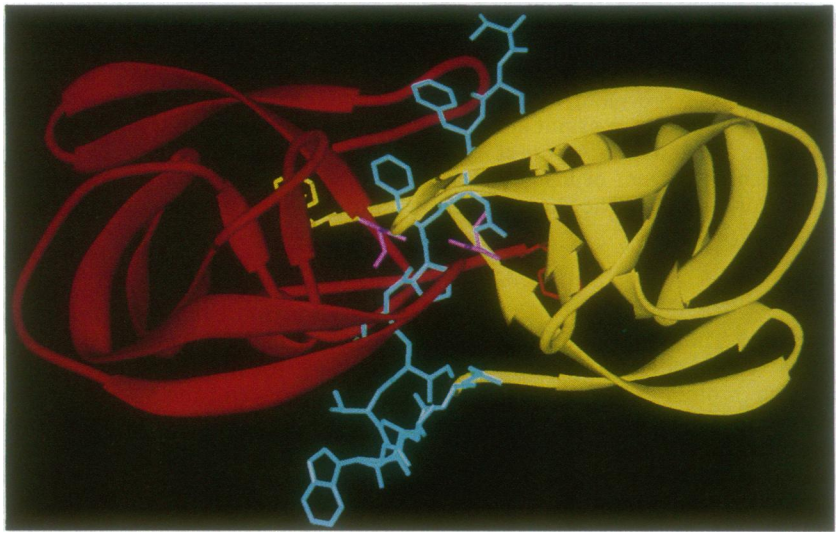

FIG. 5. Calculated structure of HIV-1 protease with ΔTF fused to the N terminus and bound to its active site. Subunits A and B, the ΔTF sequence, and the active-site aspartic residues are shown in red, yellow, light blue, and violet, respectively.

mature enzyme is produced for the intermolecular mechanism to become competitive, and (*iii*) autoprocessing occurs at an active site similar to that of the mature enzyme. On the other hand, there are some distinct differences. First, the formation of a homodimer of the protease domain is required for the HIV protease, whereas pepsinogen is a single polypeptide chain. Second, the C terminus of pepsinogen is not modified during the activation process, whereas the enzymatically active bipod further loses its C-terminal strands to generate the mature protease. Third, the tetrapod possesses much lower intrinsic protease activity than the mature enzyme, whereas pepsinogen appears to have an activity comparable to that of pepsin in the activation reaction (26). Recently, the independent expression of the N- and C-terminal domains of pepsinogen was reported (27). The two-chain pepsinogen formed by mixing equimolar amounts of the N- and C-terminal domains is activated by cleavage at its N terminus with a first-order rate constant 1.5 times that of native pepsinogen. Thus, it appears that cleavage of the scissile peptide bond at the N terminus to activate aspartic proteases from their relatively inactive precursors is a common feature that is conserved throughout the evolutionary process.

1. Skalka, A. M. (1989) *Cell* **56,** 911–913.
2. Kay, J. & Dunn, B. M. (1990) *Biochim. Biophys. Acta* **1048,** 1–18.
3. Kohl, N. E., Emini, E. A., Schleif, W. A., Davis, L. J., Heimbach, J. C., Dixon, R. A. F., Scolnick, E. M. & Sigal, I. G. (1988) *Proc. Natl. Acad. Sci. USA* **85,** 4686–4690.
4. Burstein, H., Bizub, D., Kotler, M., Schatz, G., Vogt, V. M. & Skalka, A. M. (1992) *J. Virol.* **66,** 1781–1785.
5. Louis, J. M., McDonald, R. A., Nashed, N. T., Wondrak, E. M., Jerina, D. M., Oroszlan, S. & Mora, P. T. (1991) *Eur. J. Biochem.* **199,** 361–369.
6. Fitzgerald, P. M. D. & Springer, J. P. (1991) *Annu. Rev. Biophys. Biophys. Chem.* **20,** 299–320.
7. Richards, A. D., Phylip, L. H., Farmerie, W. G., Scarborough, P. E., Alvarez, A., Dunn, B. M., Hirel, P.-H., Konvalinka, J., Strop, P., Pavlickova, L., Kostka, V. & Kay, J. (1990) *J. Biol. Chem.* **265,** 7733–7736.
8. Nashed, N. T., Louis, J. M., Sayer, J. M., Wondrak, E. M., Mora, P. T., Oroszlan, S. & Jerina, D. M. (1989) *Biochem. Biophys. Res. Commun.* **163,** 1079–1085.
9. Wlodawer, A., Miller, M., Jaskolski, M., Sathyanarayana, B. K., Baldwin, E., Weber, I. T., Selk, L. M., Clawson, L., Schneider, J. & Kent, S. B. H. (1989) *Science* **245,** 616–621.
10. Jones, T. A. (1978) *J. Appl. Crystallogr.* **11,** 268–272.
11. Hartsuck, J. A., Koelsch, G. & Remington, S. J. (1992) *Proteins Struct. Funct. Genet.* **13,** 1–25.
12. Fitzgerald, P. M. D., McKeever, B. M., VanMiddlesworth, J. F., Springer, J. P., Heimbach, J. C., Leu, C.-T., Herber, W. K., Dixon, R. A. F. & Darke, P. L. (1990) *J. Biol. Chem.* **265,** 14209–14219.
13. Satow, Y., Cohen, G. H., Padlan, E. A. & Davies, D. R. (1986) *J. Mol. Biol.* **190,** 593–604.
14. Rich, D. H. (1985) *J. Med. Chem.* **28,** 263–273.
15. Broadhurst, A. V., Roberts, N. A., Ritchie, A. J., Handa, B. K. & Kay, C. (1991) *Anal. Biochem.* **193,** 280–286.
16. Billich, A., Hammerschmid, F. & Winkler, G. (1990) *Biol. Chem. Hoppe Seyler* **371,** 265–272.
17. Krausslich, H.-G. (1991) *Proc. Natl. Acad. Sci. USA* **88,** 3213–3217.
18. Burstein, H., Bizub, D. & Skalka, A. M. (1991) *J. Virol.* **65,** 6165–6172.
19. Spurlino, J. C., Lu, G.-Y. & Quiocho, F. A. (1991) *J. Biol. Chem.* **266,** 5202–5219.
20. Creighton, T. E. (1993) *Proteins Structure and Molecular Properties* (Freeman, New York), 2nd Ed.
21. Jackson, S. E. & Fersht, A. R. (1991) *Biochemistry* **30,** 10436–10443.
22. Duplay, P., Bedouelle, H., Fowler, A., Zabin, I., Saurin, W. & Hofnung, M. (1984) *J. Biol. Chem.* **259,** 10606–10613.
23. Hyland, L. J., Tomaszek, T. A., Jr., & Meek, T. D. (1991) *Biochemistry* **30,** 8454–8463.
24. Darke, P. L., Nutt, R. F., Brady, S. F., Garsky, V. M., Ciccarone, T. M., Leu, C.-T., Lumma, P. K., Freidinger, R. M., Veber, D. F. & Sigal, I. S. (1988) *Biochem. Biophys. Res. Commun.* **156,** 297–303.
25. Navia, M. A., Fitzgerald, P. M. D., McKeever, B. M., Leu, C.-T., Heimbach, J. C., Herber, W. K., Sigal, I. S., Darke, P. L. & Springer, J. P. (1989) *Nature (London)* **337,** 615–620.
26. Marciniszyn, J., Jr., Huang, J. S., Hartsuck, J. A. & Tang, J. (1976) *J. Biol. Chem.* **251,** 7095–7102.
27. Lin, X.-I., Lin, Y.-Z., Koelsch, G., Gustchina, A., Wlodawer, A. & Tang, J. (1992) *J. Biol. Chem.* **267,** 17257–17263.